

CCN activation experiments with adipic acid: effect of particle phase and adipic acid coatings on soluble and insoluble particles

S. S. Hings¹, W. C. Wrobel¹, E. S. Cross¹, D. R. Worsnop², P. Davidovits¹, and T. B. Onasch^{1,2}

¹Department of Chemistry, Boston College, Chestnut Hill, MA 02467, USA

²Aerodyne Research Inc., Billerica, MA 01821, USA

Received: 1 February 2008 – Accepted: 1 February 2008 – Published: 4 March 2008

Correspondence to: S. S. Hings (hings@bc.edu)

Published by Copernicus Publications on behalf of the European Geosciences Union.

4439

Abstract

Slightly soluble atmospherically relevant organic compounds, such as adipic acid, may influence particle CCN activity and therefore cloud formation. The 11 published experimental studies on the CCN activity of adipic acid particles are not consistent with each other nor do they in most cases agree with the Köhler theory. The CCN activity of adipic acid aerosol particles was studied over a significantly wider range of conditions than in any previous single study. The work spans the conditions of the previous studies and also provides alternate methods for producing wet and dry adipic acid particles without the need to produce them by atomization of aqueous solutions. The CCN effect of adipic acid coatings on both soluble and insoluble particles has also been studied. The CCN activation of the small ($d_m < 150$ nm) initially dry particles is subject to a deliquescence barrier, while for the larger particles the activation follows the Köhler curve. Adipic acid particles prepared in a wet state follow the Köhler curve over the full range of particle diameters studied. The experiments suggest that the scatter in the previously published CCN measurements is most likely due to the difficulty of producing uncontaminated adipic acid particles by atomization of solutions and possibly also due to uncertainties in the calibration of the instruments. The addition of a hydrophilic soluble compound to dry adipic acid eliminates the effect of particle phase, that is, the effect of the deliquescence barrier to CCN activation. An adipic acid coating on hydrophobic soot yields a CCN active particle. For the relatively small soot particles ($d_{\text{core}} = 88$ and 102 nm) the CCN activity of the coated particles approaches the deliquescence line of adipic acid, suggesting that the total size of the particle determines CCN activation and the soot core acts as a scaffold.

1 Introduction

As has been discussed in several publications, the effect on climate of aerosol radiative forcing may be as large as that of the greenhouse gases but much more uncertain.

4440

(See for example, Kaufman and Koren, 2006; Schwartz et al., 2007; IPCC, 2007). The high uncertainties are due to the currently inadequate representation of the complex interactions of aerosols with climate and the intrinsically complex composition of aerosol particles.

5 Aerosol particles affect climate through direct and indirect interactions. Through direct effects clear air aerosols containing black carbon (BC), absorb incoming light heating the atmosphere, while most other aerosols scatter light and produce cooling. Through the indirect effect, hydrophilic aerosols may serve as cloud condensation nuclei (CCN) affecting cloud cover and hence the radiation balance. The type of cloud
10 cover formed depends in a complex way on aerosol size, composition and concentration.

Slightly soluble organics, such as adipic acid, succinic acid, and stearic acid, are atmospherically relevant compounds that may significantly influence CCN activity and thus influence the indirect effect via cloud formation. Consequently, the CCN behavior
15 of dicarboxylic acids has been studied extensively and has been found to vary widely (Cruz and Pandis, 1997; Corrigan and Novakov, 1999; Prenni et al., 2001; Giebl et al., 2002; Raymond and Pandis, 2002; Kumar et al., 2003; Bilde and Svenningsson, 2004; Broekhuizen et al., 2004; Huff Hartz et al., 2005; Rissman et al., 2007). For example, the CCN activity of oxalacetic acid is high, comparable to that of ammonium sulfate,
20 on the other hand, suberic acid is CCN inactive. While the CCN behavior of some dicarboxylic acids such as succinic acid has been successfully predicted from Köhler theory modified to include solubility and surface tension effects, published experimental studies on the CCN activity of slightly soluble adipic acid particles are in most cases not consistent with the Köhler theory and vary widely from one study to another.

25 It has been suggested and experimentally verified for several compounds (for example succinic acid and adipic acid) that particle phase plays an important role in the activation of particles consisting of slightly soluble organic compounds (Hori et al., 2003; Bilde and Svenningsson, 2004; Broekhuizen et al., 2004). Bilde and Svenningsson (2004) have also shown that small amounts of inorganic salts may have a significant

4441

effect on the percent critical supersaturation (S_c) of slightly soluble organic compounds.

1.1 Previously published S_c data for adipic acid

Figure 1 shows published adipic acid critical supersaturation data as a function of particle diameter from 11 studies. In all these experiments particles were formed by atomizing aqueous solutions of adipic acid. Particles were subsequently dried to relative humidities between 5 and 20%. In one case only, particles were kept wet as a supersaturated solution droplet (designated in the figure as “wet”). In one set of experiments Rissman et al. (2007) heated the adipic acid particles prior to drying them.

The solid lines are obtained from standard Köhler theory calculations described in Appendix A. The orange line is the calculation for adipic acid using concentration dependent surface tension. The red line is the calculation for ammonium sulfate particles and the solid black line is the Köhler curve for pure water that is a stand-in for a wettable but insoluble substance (Petters and Kreidenweis, 2007). The broken lines in the figure provide visual continuity for the experimental points.

15 As is evident from Fig. 1, the published data for adipic acid exhibit significant scatter. For example, at 1% supersaturation, measured critical diameters for adipic acid particles vary from 50 nm to 180 nm. The measurements of Bilde and Svenningsson (2004) for wet particles fall close to the traditional Köhler theory line for adipic acid. The measurements of Rissman et al. (2007) for larger sized particles approach the predictions of the Köhler theory. All other data show higher critical supersaturations than predicted by the Köhler theory. The large variations in measured supersaturation are likely caused by differences in particle preparation, as will be discussed (Rissman et al., 2007), and also possibly due to methods of CCN measurement (see Appendix B).

25 The purpose of the present work is to understand the factors governing the CCN activity of slightly soluble organic compounds and in the process explain the wide variations in the published S_c measurements for adipic acid. Toward these ends we studied the CCN activity of adipic acid aerosol over a significantly wider range of conditions

4442

then has been previously done in any single study. Our work spans the conditions of the previous studies and also provides alternate methods for producing wet and dry adipic acid particles without the need to produce them by atomization of aqueous solutions.

5 After a very short residence time in the atmosphere most aerosol particles acquire a coating of one type or another. To complete the picture of adipic acid activation, the CCN effect of adipic acid coatings on both soluble and insoluble cores has also been investigated.

2 Experimental

10 2.1 Apparatus

A schematic diagram of the experimental apparatus is shown in Fig. 2. The main components of the set-up are: A particle generation system, a particle coating system, two differential mobility analyzers (DMA I, TSI Model 3071A, and DMA II, TSI Model 3080), a condensation particle counter (CPC, TSI Model 3010), a continuous-flow stream-
15 wise thermal-gradient CCN counter (CCNC, Droplet Measurement Technologies), and a Time-of-Flight Aerosol Mass Spectrometer (ToF-AMS, Aerodyne Research Inc.).

With the exception of the CCNC apparatus, all instruments used are either standard aerosol instrumentation or in case of the ToF-AMS are described in detail in the literature (Drewnick et al., 2005, DeCarlo et al., 2006). Because the CCNC apparatus is
20 a relatively new addition to the field of aerosol science, this instrument is described briefly in the following section.

2.1.1 Cloud Condensation Nuclei Counter (CCNC)

The DMT (Droplet Measurement Technologies) CCN counter used in this study is operated in a continuous flow mode. That is, the instrument continually monitors the

4443

CCN activity of the particles passing through the instrument. This mode of operation provides fast sampling. The instrument is capable of generating along the centerline nearly constant values of supersaturation between 0.07% and 3.7% with a stated accuracy of $\pm 2\%$. Supersaturation is easily controlled and maintained, making it possible
5 to scan the full range of supersaturation for a given particle size.

The aerosol flow introduced into the instrument is split into an aerosol and a sheath flow. The sheath flow is filtered, humidified and heated, and constrains the main aerosol flow to the centerline of the cylindrical CCN column. The inner wall of the CCN column is continually wetted and a positive temperature gradient dT is applied to
10 the CCN column in the direction of the flow. Water vapor supersaturation is therefore generated along the centerline of the CCN column. Particles begin to grow at the point where the supersaturation is equal to S_c . Droplets that grow to diameters larger than $1 \mu\text{m}$ are detected by an optical particle counter (OPC) at the exit of the column.

The supersaturation in the CCN column is primarily a function of the temperature difference dT between the top (upstream) and the bottom (downstream) of the CCN column. It also depends on the flow and the pressure inside the instrument. The relationship between supersaturation S and the measured temperature difference dT inside the CCN column is determined by calibration with ammonium sulfate particles
15 at a specific flow and pressure. To obtain reliable experimental results the CCNC apparatus has to be carefully calibrated in each specific application.

For a detailed description of the CCNC and its calibration, refer to Roberts and Nenes (2005), Lance et al. (2006), and Rose et al. (2007). Specific details relevant to our measurements are presented in Appendix B.

2.2 Experimental procedures

25 As was stated, in all the previous studies the adipic acid particles were generated by atomization of aqueous adipic acid solutions. In order to explore the full range of experimental conditions, we generated particles both by atomization and by condensation of adipic acid vapor. The following measurements were performed to study the CCN

4444

activity of adipic acid. 1) CCN activity of dry adipic acid particles generated by atomization. 2) CCN activity of dry adipic acid generated by homogeneous nucleation. 3) CCN activity of wet adipic acid particles generated by atomization. 4) CCN activity of wet adipic acid particles generated by vapor deposition of adipic acid on a small ammonium sulfate core (this method of generating wet adipic acid is discussed in detail). 5) CCN activity of adipic acid coated on ammonium sulfate particles studied as a function of coating thickness. 6) CCN activity of adipic acid coated on soot particles as a function of coating thickness.

2.2.1 Particle generation

The methods of generating particles for the 6 studies listed above are in order. If particles are to be dried they are passed through diffusion driers as shown in Fig. 2. The particles are size-selected by DMA I and, if they are to be coated they are passed through the coating reservoir which can be bypassed.

1. An aqueous solution of adipic acid in water is atomized to generate supersaturated solution droplets. The aerosol flow is then heated ($\sim 60^{\circ}\text{C}$) and passed through three diffusion driers filled with silica gel.

2. Adipic acid particles are generated via homogeneous nucleation of adipic acid. Adipic acid is heated in a round bottom flask to approximately 150°C . The airflow through the nucleation region is 2 L/min. The particles nucleate as the flow is passed through a cooled region. This method provides pure dry (solid) adipic acid particles.

3. An aqueous solution of adipic acid in water is atomized to generate supersaturated solution droplets. The aerosol flow is not dried and the DMA sheath flow is humidified.

4445

4. Adipic acid is dry-vapor deposited onto a small dried ammonium sulfate core. Ammonium sulfate particles are generated by atomization of an aqueous solution and subsequently dried by passing them through a diffusion drier filled with anhydrous calcium sulfate (Drierite). The particles are then size-selected by DMA I and passed through a region containing the heated adipic acid reservoir. In this region, the ammonium sulfate particles become coated by adipic acid upon vapor deposition.

On entering the CCN column, the highly water-soluble ammonium sulfate core absorbs enough water to completely dissolve the adipic acid forming a concentrated adipic acid ammonium sulfate aqueous solution. We postulate that water reaches the ammonium sulfate core either via diffusion through the adipic acid coating or by passage through imperfections in the coating. Experiments as well as calculations (Appendix A) show that if the mass fraction of the ammonium sulfate core is small ($<15\%$), this method provides an aerosol particle that can be considered to be a single-component "wet" adipic acid particle.

5. For these experiments, adipic acid is coated onto ammonium sulfate cores as described above.

6. Soot particles are generated by combustion of ethylene and oxygen in a commercial McKenna burner (Slowik et al., 2004), and passed through a diffusion drier filled with activated carbon to remove flame-generated organics. The particles are then size-selected and coated by vapor deposition of adipic acid.

25

4446

2.2.2 Measurement of particle CCN activity

After particle generation and size-selection, the aerosol flow is split with one part directed into the DMA II and the other into the ToF-AMS. Before and after each CCN experiment (i.e., every time a new particle size is selected), the second DMA and the CPC are used as a scanning mobility particle sizer (SMPS) to measure the size distribution of the particles. During a CCN experiment the particles are size-selected a second time with DMA II in accord with the mode diameter determined during the SMPS scan. When the particles are simply pure adipic acid the mode diameter is the diameter selected with DMA I. When the particles are coated, the DMA II measures the new diameter of the coated particles. The resulting monodisperse aerosol flow exiting DMA II is split between the CCNC and the CPC.

The supersaturation in the CCNC is varied between 0.07% and 3.7% by setting the CCN instrument dT between 1.5 and 27 K. During all experiments, the CCNC was operated at a total flow rate of 1 L/min.

The fraction of CCN activated aerosol is the ratio of the number concentration of CCN measured by the CCNC (N_{CCN} , i.e. all particles that grow larger than $1 \mu\text{m}$ detected by the OPC) to the total number concentration of particles measured by the CPC (N_{CPC}). The critical supersaturation S_c at a particular aerosol size is defined as the supersaturation at which 50% of the particles grow into droplets (activated fraction = $\frac{N_{CCN}}{N_{CPC}} = 0.5$).

Figure 3 shows an example of activation curves measured for ammonium sulfate particles of two diameters; 45 nm and 31 nm. Such curves are generated by measuring the fraction of activated aerosol and plotting this number as a function of the temperature difference dT in the CCNC column. The plot is fitted with a sigmoid function to find the critical temperature difference dT_c where the activated fraction is 0.5. The critical supersaturation S_c is then calculated from the calibration curve described in Appendix B. The width of the sigmoidal curve is due to the spread in the aerosol size distribution determined by the DMA transmission function.

4447

2.2.3 Determination of the particle shape factor

The methods of aerosol generation may produce particles that are not spherical. Tandem DMA-AMS measurements, where particles are selected by mobility and then sized aerodynamically, can be used to obtain information about particle shape. This procedure is described in detail in DeCarlo et al. (2004) and Slowik et al. (2004).

The general expression for relating d_{va} and d_m measurements is:

$$\frac{\frac{d_{va} \chi_v \chi_t \rho_0}{\rho_p}}{C_c \left(\frac{d_{va} \chi_v \rho_0}{\rho_p} \right)} = \frac{d_m}{C_c(d_m)} \quad (1)$$

Here, χ_v and χ_t are the dynamic shape factors in the free molecular and the transition regime, ρ_0 is unit density, ρ_p is the particle density, and $C_c(d)$ is the Cunningham slip correction factor. If one assumes that $\chi_t = \chi_v$ then for a known particle density ρ_p (which is equal to ρ_m for particles without internal voids), the dynamic shape factor χ of the particles can be estimated (DeCarlo et al., 2004).

3 Results and discussion

3.1 Overview

In accord with the particle generation methods described in Sect. 2.2.1, the results of the following measurements are presented and discussed in this section. 1) CCN activation of dry adipic acid particles generated by atomization followed by drying. 2) CCN activation of dry adipic acid particles generated by homogeneous nucleation of adipic acid vapor. 3) CCN activity of wet adipic acid particles generated by atomization. 4) CCN activity of wet adipic acid particles generated by vapor deposition of adipic acid on a small ammonium sulfate core (see Sect. 2.2.1). 5) CCN activity of adipic acid coated on ammonium sulfate particles studied as a function of coating thickness. 6)

4448

CCN activity of adipic acid coated on soot particles as a function of coating thickness. The experimental results are discussed in the framework of the modeling calculations described in Appendix A.

Appendix A presents modeling calculations relevant to the experimental studies. The following summarizes the topics presented in Appendix A. (a) Standard Köhler theory including the effect of the solute on the surface tension of the aqueous solution. (b) Modified Köhler theory. The standard Köhler theory is applicable to completely dissolved aqueous solutions (i.e.: a solution of adipic acid dissolved in water or ammonium sulfate dissolved in water). In the present work, the activation of ammonium sulfate particles coated by adipic acid is also studied. In such a case the particle may contain an undissolved adipic acid core surrounded by a solution of water, adipic acid and ammonium sulfate. Shulman et al. (1996) and Laaksonen et al. (1998) modified the standard Köhler theory to describe the CCN activation of such aerosol particles. As is shown in the Appendix, in our experiments the standard Köhler theory is applicable in all cases. Further, the theory shows that as long as the mass fraction of the adipic acid is higher than 0.85, the effect of ammonium sulfate on the CCN activity of the particle is less than 10%. This result validates the method of generating the wet adipic acid particles by vapor deposition of adipic acid on a small ammonium sulfate core. (c) Deliquescence-controlled activation of organics. A solid compound must first deliquesce before it can become CCN active. The water vapor pressure required for a particle to deliquesce is expressed in terms of the ratio S_{del} of the deliquescent water vapor pressure to the equilibrium pressure. As is evident from Eq. (A8), S_{del} increases exponentially with decreasing particle diameter. When $S_{del} > S_c$, activation is governed by S_{del} . In other words, in this region deliquescence is the barrier to activation. For $S_{del} < S_c$ CCN activation is governed by the Köhler theory.

The experimental studies described here fall into two categories: Single component adipic acid studies (1, 2, 3 and 4) and adipic acid coating studies (5 and 6).

4449

3.2 Single-component adipic acid

3.2.1 Results of experiments with dry adipic acid particles generated by atomization

We conducted a wide range of CCN activation experiments with adipic acid particles generated by atomization of adipic acid solutions followed by drying. About 15 such independent experimental CCN activation experiments were conducted. We were not able to obtain from day to day consistently reproducible data sets with adipic acid aerosols produced by atomization, nor were we able to ascertain the cause of this irreproducibility. Most likely the scatter in the data is due to trace impurities in the solution which we were not able to completely eliminate in spite of our best efforts.

3.2.2 Results of experiments with dry adipic acid particles obtained by homogeneous nucleation

The results of CCN activation experiments with dry adipic acid particles produced by homogeneous nucleation of adipic acid vapor are shown in Fig. 4 as blue points. Here the measured critical supersaturation S_c is shown as a function of dry particle diameter d_d . The data are the results for each point of at least 3 independent measurements performed over a period of 3 days. The broken line provides visual continuity for the measured points. The standard deviation of the measurements as indicated by the error bars is in all cases but one less than 4%. As is evident, the vapor-nucleation method of producing adipic acid particles produces consistent results with little scatter. The solid lines are the same calculated Köhler lines shown in Fig. 1. The shaded area models the deliquescence of the particles according to the Kelvin Eq. (A8) as discussed in Appendix A. The surface tension of saturated aqueous adipic acid droplets larger than 40 nm is calculated to have values between 0.060 and 0.072 J/m² (See Eq. (A4)). A water activity over a saturated adipic acid solution of $\gamma_w = 0.99$ was chosen to provide a best fit to the experimental data. The borders of the shaded region are obtained with the two limiting values of calculated surface tension. Deliquescence modeling lines for

4450

other values of γ_w are shown in Appendix A.

As is evident, the CCN activities of particles smaller than 150 nm in diameter are not governed by the Köhler theory. The activation of the smaller particles more closely follows the predictions of the deliquescence calculations, although the fit is not fully precise. Still, the general trend in the measurements follows the deliquescence model, supporting the suggestion of Hori et al. (2003) and Kreidenweis et al. (2006) that deliquescence-controlled activation may govern droplet formation for small, slightly soluble particles. The smallest particle ($d_{\text{mob}}=88$ nm) in this set of measurements behaves as a particle composed of an insoluble wettable material. (This size was the smallest for which we were able to obtain accurate results.) The activation of particles larger than ~ 150 nm follows Köhler theory.

As described in Sect. 2.2.3, the dynamic shape factor χ of the particles can be estimated from DMA/AMS size measurements. Using an adipic acid density of 1.36 g/cm^3 , we estimate the dynamic shape factors to be as shown in Table 1. The uncertainties in χ are primarily due to the uncertainty in $d_{v,a}$, which is approximately $\pm 15\%$. Within these error limits, we cannot state whether the particles deviate significantly from a spherical shape.

4451

Comparison with previous studies

In Fig. 5 we once again show the previously published CCN activation data for dry adipic acid aerosol, this time together with our measurements using nucleation-generated particles. As is evident, some of the S_c measurements are above and some are below our values. The wide scatter in the measured CCN activity obtained in the previous studies suggests that some significant parameter or parameters vary from experiment to experiment. Our experiments do not provide an explanation for these discrepancies, however we can suggest some possible factors that may affect the results. Because all the previous experiments were performed with aerosol generated by atomization, we suggest that solution impurities are one possible cause of the scatter in the data. We note that all the previously obtained S_c results fall above the Köhler curve. That is, they are all in the region where deliquescence governs the onset of activation. Therefore, if impurities are the cause of the scatter, they must be such that some promote and others hinder particle deliquescence.

Another possible reason for the scatter in the previous measurement of S_c may be due to the shape of the particles produced by the atomization/drying process. The volume-equivalent diameter $d_{v,e}$ of a non-spherical particle is smaller than its electrical mobility diameter d_m (DeCarlo et al., 2004). In all the previous measurements the quoted diameter is the mobility diameter as measured by a DMA instrument. If in fact the atomizing-generated particles are non-spherical, their effective diameter is smaller than d_m and the points to the right of our data would be shifted to the left, closer to the results obtained in our studies. A possible confirmation of this hypothesis is provided by the data of Rissman et al. (2007). They show data for particles that were additionally heated. These data fall to the left of their unheated particle measurements. This might be due to a reconfiguration of the adipic acid upon heating, resulting in a more spherical shape of the particles.

As is shown in Appendix B the calibration of the CCN instrument is a critical part of these experiments. Variations in the calibration of the CCN instrument from one

4452

experimental group to another cannot at this point be ruled out as one of the causes for the scatter in the data.

3.2.3 Wet adipic acid

As is shown in Fig. 1, there is only one previously published CCN activation study for wet adipic acid aerosol particles. The results of this study are in agreement with the Köhler theory. As we stated earlier, we were not able to obtain consistent measurements with either wet or dry adipic acid aerosol produced by atomization. Most of our wet adipic acid measurements, resulting from 5 independent runs, fell below the critical supersaturation predicted by the Köhler theory. We attribute the scatter in these data to residual impurities, most likely ammonia, which can play a role in experiments with wet adipic acid. The CCN activity of initially dry adipic acid however is reported to be unaffected by ammonia (Dinar et al., 2008).

To eliminate possible impurities we generated wet adipic acid aerosol by coating small ammonium sulfate cores with adipic acid mass fractions greater than 0.85.

Experiments were conducted with three ammonium sulfate core sizes ($d_{\text{core}}=34$ nm, 53 nm, 73 nm) coated with adipic acid. In this subset of experiments, the adipic acid mass fraction was in all cases greater than 0.85. As discussed in Sect. 2.2.1, under these conditions the CCN activity of the particle is determined to within 10% by adipic acid. The results are shown in Fig. 6 together with the previously measured values for wet adipic acid obtained by Bilde and Svenningsson (2004). As is evident, the data are in accord with the Köhler theory. The 5 to 10% expected effect on S_c of the dissolved ammonium sulfate core is not evident on the scale of the figure.

4453

3.3 Adipic acid coating experiments

3.3.1 Ammonium sulfate coated with adipic acid

In the coating studies three ammonium sulfate particles of three sizes ($d_{\text{core}}=34$, 53 and 73 nm) were coated with adipic acid (coating thickness ~ 5 –34 nm), and the CCN activity was measured as a function of the total particle size (ammonium sulfate core + adipic acid coating). The results are shown in Fig. 7 as plots of S_c as a function of total particle diameter. The solid orange and red lines in the figure are as before the Köhler curves for pure adipic acid and pure ammonium sulfate, respectively. The dotted lines are results of calculations using Köhler theory, taking into account the combined activity of the solution (see Appendix A).

As is evident in each case the CCN activity of the uncoated ammonium sulfate particle falls on the ammonium sulfate Köhler line even though the particle is initially a dry solid. The initial solid phase of the particle does not hinder activation because ammonium sulfate deliquesces readily and the water vapor pressure in the CCNC instrument is always above the deliquescence vapor pressure for ammonium sulfate. As expected, with increasing adipic acid coating thickness, the measured S_c values rise above the ammonium sulfate Köhler line and approach the adipic acid Köhler line as the adipic acid mass fraction rises above 0.85. These endpoints in the adipic acid coating studies are the S_c data in Fig. 6.

We note, that the vapor deposited adipic acid coating is initially a dry solid. The above results indicate that the addition of a hydrophilic soluble compound to dry adipic acid eliminates the effect of particle phase, that is, the effect of the deliquescence barrier to CCN activation.

3.3.2 Soot coated with adipic acid

In this set of coating experiments four soot particles of sizes $d_{\text{core}}=88$ nm, 102 nm, 136 nm and 181 nm were coated with adipic acid, and the CCN activity was measured as

4454

a function of the adipic acid coating thickness (<3–75 nm). These experiments were performed to test the effect on CCN activity of adipic acid coatings on an insoluble hydrophobic core. (The uncoated soot particles of the sizes studied are CCN inactive in the supersaturation range of 0.07–3.7%.)

5 Figure 8 shows the measured critical supersaturations as a function of the total particle diameter (soot core + adipic acid coating). Our CCN activation measurements for dry adipic acid particles are included for comparison.

While the uncoated soot particles are CCN inactive, even very thin coatings (~<3 nm), triggers CCN activity. These initial points are at the tops of the activation lines, corresponding to the calculated critical supersaturations S_c of a wettable solid core.

As shown in the figure, for the smaller soot cores ($d_{\text{core}}=88$ nm and 102 nm), the measured critical supersaturations approach those measured for dry adipic acid, suggesting that the particles activate at the deliquescence relative humidity (DRH) (S_{del}) of adipic acid and the soot cores act as scaffolds for the organic compound. Here, the total size of the particle governs DRH and CCN activity, not the overall composition of the particle.

The S_c measurements for the larger soot core sizes ($d_{\text{core}}=136$ and 181 nm) are displaced to the right of the dry adipic acid line indicating a lower CCN activity relative to the smaller particles. This observation seems to suggest that in the case of larger coated soot particles the soot core does not act simply as a scaffold for the coating. It appears that the effective CCN diameter of the larger coated soot is smaller than the particle diameter. We can suggest a possible reason for this obvious difference between the CCN behavior of the larger and smaller coated soot particles.

25 Because the soot itself is hydrophobic, water interacts only with the adipic acid coated onto the soot. Therefore, only the diameter of the adipic acid coating influences the CCN activity of the coated particle (effective diameter). It is possible that the small soot cores are coated more evenly than the larger cores. An even coating yields an effective diameter equal to the total particle diameter. On the other hand, an

4455

uneven coating may produce adipic acid “islands” with effective diameter that is smaller than the total particle diameter. While other mechanisms related to shape and fractality factors that would result in smaller effective particle diameters could be suggested, the S_c measurements for the larger soot particles remain unexplained.

5 4 Conclusions

The CCN activity of both dry and wet adipic acid particles, and the effect of adipic acid coatings on the CCN activity of soluble and insoluble particles were determined. The results of the experiments lead to the following conclusions:

1. In accord with earlier suggestions (Hori et al., 2003, and Kreidenweis et al., 2006) the CCN activation of the small ($d_m < 150$ nm) slightly soluble initially dry particles is governed by deliquescence ($S_{\text{del}} > S_c$). For the larger particles, where $S_{\text{del}} < S_c$ the activation follows the Köhler curve. As expected, adipic acid particles prepared in a wet state likewise follow the Köhler equation.
2. The scatter in the previously published experiments remains unexplained. Possible factors causing the scatter are suggested.
3. The experiments with adipic acid coated ammonium sulfate aerosol particles indicate that the addition of a hydrophilic soluble compound to dry adipic acid eliminates the effect of particle phase, that is, the effect of the deliquescence barrier to CCN activation.
- 20 4. An adipic acid coating on hydrophobic soot yields a CCN active particle. For the relatively small soot particles ($d_{\text{core}}=88$ and 102 nm) the CCN activity of the coated particles approaches the deliquescence line of adipic acid, suggesting that the total size of the particle determines CCN activation and the soot core acts as a scaffold. It appears that the effective CCN diameter of the larger coated soot is smaller than the particle diameter.

4456

Appendix A

Modeling CCN activity of particles

A1 Köhler theory

5 A1.1 Derivation of critical supersaturation

Standard Köhler theory provides an expression for the equilibrium water vapor pressure over an aqueous solution droplet and yields the supersaturation ratio S_w (Pruppacher and Klett, 1997):

$$S_w = \frac{p}{p_0} = \gamma_w x_w \exp\left(\frac{4M_w \sigma}{RT \rho_w d_p}\right) \quad (\text{A1})$$

10 Here, p is the vapor pressure of water over the solution droplet, p_0 is the equilibrium vapor pressure over a flat surface, γ_w is the activity of water, x_w is the mole fraction of water in the aqueous solution, M_w is the molar mass of water, σ is the surface tension of the solution droplet, R is the universal gas constant, T is the temperature, ρ_w is the density of water, and d_p is the diameter of the droplet at water vapor pressure p . This diameter will be designated as the “wet” diameter.

15 The $\gamma_w x_w$ term represents the Raoult (or solution) effect, which increases with increasing wet diameter d_p . The exponential term represents the Kelvin (or curvature) effect, and it decreases with increasing wet diameter. These two competing effects result in a maximum with respect to d_p for Eq. (A1).

20 The term commonly used to describe particle growth by vapor condensation is supersaturation S in % defined as

$$S = (S_w - 1) \cdot 100 \quad (\text{A2})$$

Figure A1 displays S as a function of the wet particle diameter d_p . The maximum of this curve is known as the critical supersaturation (S_c). An aerosol particle is CCN active (i.e. grows into a cloud droplet) if supersaturation exceeds this maximum.

25 4457

Standard Köhler theory is used to describe the activation of single-component aqueous solution droplets and is used here to model ammonium sulfate and completely dissolved adipic acid.

A1.2 Surface tension

5 As is evident from Eqs. (A1) and (A3), surface tension is a key parameter for the calculation of S_w and therefore S_c . It has been shown that dissolved surface active slightly soluble organic compounds lower the surface tension of aqueous solutions, depending on concentration, by as much as one third (Shulman et al., 1996; Facchini et al., 2000). A decrease in σ lowers the critical supersaturation as predicted by Köhler theory.

10 The surface tension of an adipic acid solution can be calculated from the Szyszkowski-Langmuir equation as has been done by Henning et al. (2005):

$$\sigma = \sigma_w(T) - aT \ln(1 + bC) \quad (\text{A3})$$

Here, C is the concentration of dissolved carbon in moles of carbon per kg of water and $\sigma_w(T)$ is the surface tension of water at temperature T . The parameters a and b are obtained by fitting the experimental results to Eq. (A3). For pure adipic acid, Henning et al. (2005) obtained for $a=0.0264$ and $b=0.286$.

A1.3 Results of S_c calculations

Using Eqs. (A1) and (A2), critical supersaturations S_c were calculated as a function of initially dry particle diameter for three substances: Ammonium sulfate, adipic acid and an insoluble but wettable substance (See Fig. A2). Ammonium sulfate is modeled using the surface tension of water (0.072 J/m^2). Adipic acid is modeled with both the concentration-dependent surface tension defined by the Szyszkowski-Langmuir equation (Eq. (A3)) and the surface tension of water (0.072 J/m^2). The black line in Fig. A2 is the critical supersaturation for a pure water droplet. This effectively models the growth of an insoluble but wettable spherical surface and is hereafter referred to as “wetable line”.

25 4458

A2 Modified Köhler theory for adipic acid particles containing a highly soluble core

The Köhler theory as described by Eqs. (A1) and (A2) is applicable for completely dissolved aqueous solutions (that is, a solution of adipic acid dissolved in water or ammonium sulfate dissolved in water). In the present work, the activation of ammonium sulfate particles coated by initially dry adipic acid is also studied. In such a case the possibility exists that the droplet contains an undissolved adipic acid core surrounded by a solution of water, adipic acid, and ammonium sulfate. The presence of the ammonium sulfate allows condensational growth of the particle by addition of water without causing the complete deliquescence of the adipic acid. Shulman et al. (1996) modified the standard Köhler theory to describe such a situation on the activation of an aerosol particle into a cloud droplet. The presence of such a slightly soluble core that gradually dissolves as the droplet grows due to water condensation modifies the overall shape of the Köhler growth curve.

To develop the required modified Köhler theory it is convenient to approximate Eq. (A1) by an expression valid for particles larger than 30 nm, (which is the case in all our studies). Assuming a water activity γ_w of unity the approximate expression is (Pruppacher and Klett, 1997):

$$S_w \approx 1 + \frac{a_w}{d_p} - \frac{b_s}{d_p^3} \quad \text{where } a_w = \frac{4\sigma M_w}{RT\rho_w} \text{ and } b_s = \frac{6M_w v_s n_s}{4\pi\rho_w} \quad (\text{A4})$$

The term v_s is the van't Hoff factor for s and n_s is the number of moles of s . In Eq. (A4), the a_w term represents the Kelvin effect while the b_s term represents the Raoult effect.

Following Laaksonen et al. (1998), droplet activation of a particle containing a soluble inorganic salt and a slightly soluble organic compound is described by:

$$S_w \approx 1 + \frac{a_w}{d_p} - \frac{b_s}{d_p^3 - d_{ss}^3} - \gamma_{ss} \quad (\text{A5})$$

Here, the undissolved core of diameter d_{ss} is incorporated in the Raoult term for the

4459

soluble salt and the γ_{ss} term accounts for the additional dissolved slightly soluble (ss) substance. Before complete dissolution of the slightly soluble core, γ_{ss} is defined as:

$$\gamma_{ss} = \frac{M_w}{M_{ss}} v_{ss} \Gamma \quad (\text{A6})$$

and after the slightly soluble core has dissolved as:

$$\gamma_{ss} = \frac{v_{ss} M_w \Gamma n_w^0}{M_{ss} n_w} \quad (\text{A7})$$

Here, v_{ss} and M_{ss} are the van't Hoff factor and the molecular weight of the slightly soluble substance, Γ is the water solubility (g/L) of the slightly soluble substance, n_w is the number of moles of water, and n_w^0 is the number of moles of water necessary to dissolve all of the slightly soluble substance. A solubility of 25 g/L for adipic acid is used as reported by Saxena and Hildemann (1996).

As pointed out by several authors (see for example Shulman et al., 1996; Laaksonen et al., 1998), the presence of an undissolved core results in two maxima leading to two supersaturation regimes on the Köhler growth curve; SS_c1 while the core is dissolving, and SS_c2 , where the core has completely dissolved. When the core is completely dissolved, the growth curve is described by the standard Köhler theory. When the peak of the SS_c1 regime is higher than that of the SS_c2 regime, modified Köhler theory predicts a higher critical supersaturation than standard Köhler theory. This case typically occurs when the particle is composed of a large amount of significantly less soluble substance than the amount of soluble inorganic salt. On the other hand if the peak of the SS_c2 regime is higher, the critical supersaturation predicted from modified Köhler theory is the same as the predictions of the standard Köhler theory. In the latter situation the slightly soluble substance is completely dissolved at the particle CCN activation. (In this case the aerosol particle is an aqueous mixture of both components.) This situation is displayed in Fig. A3.

Based on the above results it is shown, that if the solute mass fraction of adipic acid in an aqueous solution of adipic acid and ammonium sulfate is greater than 0.85, the

4460

modified and standard Köhler theories yield within 10% the same CCN activation results. The calculations therefore validate the solvent-free method for the generation of deliquesced (“wet”) adipic acid droplets (adipic acid vapor deposition on an ammonium sulfate core).

5 A3 Role of particle phase in activation of single-component organic aerosols

Bilde and Svenningsson (2004) studied the role of phase in the CCN activation of adipic acid particles and found that deliquesced (“wet”) adipic acid droplets activate at lower S_c than initially dry adipic acid particles. Kreidenweis et al. (2006) suggested that below a certain particle diameter deliquescence of initially dry organic compounds of low water-solubility occurs at higher water vapor pressure than the critical supersaturation for CCN activation. In such a case, there is an activation barrier to the onset of cloud droplet growth governed by the deliquescence of the organic species (Hori et al., 2003, and Broekhuizen et al. 2004). Therefore, two CCN activation regimes are identified for particles composed of dry slightly soluble compounds. For larger particles, CCN activation is governed by the Köhler theory. For relatively smaller particles the CCN growth is governed by deliquescence pressure ratio, given by (Pruppacher and Klett, 1997):

$$\frac{p}{p_0} = \gamma_w \exp\left(\frac{4\sigma_{\text{sat}}M_w}{d_d\rho_wRT}\right) \quad (\text{A8})$$

Here, σ_{sat} the surface tension of the saturated droplet, and d_d the dry particle diameter.

20 The % deliquescence supersaturation S_{del} is obtained in a way analogous to Eq. (A2). For smaller particles and certain single-component low water-soluble organic aerosols (including adipic acid) the parameter S_{del} can be larger than the predicted critical supersaturation S_c calculated via Eqs. (A1) and (A2). When $S_{\text{del}} > S_c$, cloud-droplet activation is controlled by the deliquescence of the particles and activation occurs when the water vapor pressure is high enough to cause particle deliquescence, that is, CCN activation occurs at S_{del} . However, when the condition is reached such that $S_{\text{del}} < S_c$,

4461

cloud-droplet activation occurs at S_c . In short, a single-component adipic acid aerosol will only activate as a CCN after the particle has deliquesced.

Figure A4 shows critical supersaturations S_c as a function of dry particle diameter calculated from Eq. (A8) using water activities of $\gamma_w=0.990$ and $\gamma_w=0.997$. As is evident from the figure, the S_c vs. dry particle diameter is strongly dependent on γ_w . For example, at $S_c=0.3\%$, a particle with a water activity of 0.990 will deliquesce at 165 nm whereas a particle with a water activity of 0.997 will deliquesce at diameter 298 nm.

Reliable activity data for adipic acid are not available and therefore activity must be calculated based on solubility and molecular weight. Using a bulk solubility of 25 g/L, Kreidenweis et al. (2006) calculated the activity coefficient of adipic acid to be 0.997. The quoted solubility is accurate to only two figures. Therefore, the activity coefficient is not likely to be more accurate. An activation coefficient of 0.99 was used in Fig. A4 in order to best fit the experimental results using the two limits of surface tension quoted in the text. (σ between 0.060 and 0.072 J/m²). See Fig. 4.

15 Appendix B

CCN instrument calibration

To perform reliable CCN activation measurements requires an accurate knowledge of the relationship between the temperature difference dT along the CCNC column and the supersaturation S . This relationship is determined by calibration, using a well-characterized highly soluble inorganic salt, such as $(\text{NH}_4)_2\text{SO}_4$ or NaCl. Previous studies have reported a linear relationship between instrument dT and S at a flow rate of 0.5 L/min for $dT > 3$ K. For smaller dT the relationship becomes nonlinear (Rose et al., 2007; Droplet Measurement Technologies, 2004). In order to obtain a larger range of supersaturations, we operate the instrument at a higher flow rate up to 1.0 L/min. We calibrated the CCN instrument at higher flow rates between 0.5 L/min and 1 L/min.

The calibration arrangement is similar to that shown in Fig. 2. Calibration was done

4462

with ammonium sulfate aerosol particles generated by atomization of an aqueous solution of $(\text{NH}_4)_2\text{SO}_4$. The particles were dried to a relative humidity (RH) $<10\%$ by passing the aerosol flow through diffusion driers. A narrow monodisperse size distribution ($d_m \pm 10\%$) was obtained by passing the particles through two Differential Mobility Analyzers (DMA I and DMA II). The aerosol flow was divided between the CCNC instrument and the condensation particle counter (CPC). Note that the CCNC counts the number of activated particles, while the CPC counts the total number of particles in the flow.

The following method was used to calibrate the CCNC instrument. Ammonium sulfate particles of a specific size (d_m) flowed into the CCNC and CPC instruments. At a set value of dT both the CCNC and the CPC particle counts were recorded. The value of dT was systematically varied. Equilibration time between dT settings was about 1 min. The value of the critical dT (dT_c) was recorded. (dT_c is the temperature difference at which 50% of the particles are activated.) Alternately, dT can be kept constant while the particle diameter is systematically varied. Again, the dT_c and the corresponding particle size are recorded. The two methods yield similar results. The critical supersaturation (S_c) was calculated for each particle size using standard Köhler theory (Eqs. (A1) and (A2)). In this way, S_c vs. dT_c calibration plots for the CCNC instrument are obtained.

The results of calibrations for flow rates of 0.93 L/min and 1 L/min are shown in Figs. B1 and B2. These were the two flow rates used in our experiments. The nonlinear part of the curve was fitted to a power function:

$$S_{c,0} = y_0 + A \cdot dT^x \quad (\text{B1})$$

Here, $S_{c,0}$, A and x are parameters determined by the fit.

As is evident, the calibration curves at both flow rates are nonlinear for $dT < 5$ K. In fact, over the range of flow rates studied the transition into the nonlinear region is unchanged at $dT < 5$ K. As was stated, some earlier measurements found the nonlinear portion of the calibration curve for $dT < 3$ K, implying that the calibration is instrument specific.

4463

While the transition to the nonlinear portion of the calibration curve is independent of the flow rate, the slopes of the linear part of the curve are a sensitive function of the flow rate as is evident in the figures. For a flow rate of 0.93 L/min the slope is 0.106%/K, for a flow rate of 1 L/min it is 0.149%/K.

In the time period of the CCN experiments (~ 8 months) the calibration was periodically repeated and was found to remain constant.

Acknowledgements. This research was supported by the Office of Science (BER), Department of Energy (Atmospheric Science Program) grant No. DE-FG02-05ER63995 and the Atmospheric Chemistry Program of the National Science Foundation (NSF) grant No. ATM-0525355. The author ESC was funded by the NASA Earth System Science Fellowship program. We thank S. Kreidenweis for helpful discussions.

References

- Bilde, M. and Svenningsson, B.: CCN Activation of Slightly Soluble Organics: The Importance of Small Amounts of Inorganic Salt and Particle Phase, *Tellus*, 56 B, 128–134, 2004.
- Broekhuizen, K., Kumar, P. P., and Abbatt, J. P. D.: Partially soluble organics as cloud condensation nuclei: Role of trace soluble and surface active species, *Geophys. Res. Lett.*, 31, L01107, doi:10.1029/2003GL018203, 2004.
- Cruz, C. N. and Pandis, S. N.: A Study of the Ability of Pure Secondary Organic Aerosol to act as Cloud Condensation Nuclei, *Atmos. Environ.*, 31, 2205–2214, 1997.
- Corrigan, C. E. and Novakov, T.: Cloud Condensation Nucleus Activity of Organic Compounds: A Laboratory Study, *Atmos. Environ.*, 33, 2661–2668, 1999.
- DeCarlo, P. D., Slowik, J. G., Worsnop, D. R., Davidovits, P., and Jimenez, J. L.: Particle Morphology and Density Characterization by Combined Mobility and Aerodynamic Diameter Measurements, Part 1: Theory, *Aerosol Sci. Tech.*, 38, 1185–1205, doi:10.1080/027868290903907, 2004.
- DeCarlo, P. F., Kimmel, J. R., Trimborn, A., Northway, M. J., Jayne, J. T., Aiken, A. C., Gonin, M., Fuhrer, K., Horvath, T., Docherty, K., Worsnop, D. R., and Jimenez, J. L.: Field-Deployable, High-Resolution, Time-of-Flight Aerosol Mass Spectrometer, *Anal. Chem.*, 78, 8281–8289, 2006.

4464

- Dinar, E., Anttila, T., and Rudich, Y.: CCN Activity and Hygroscopic Growth of Organic Aerosols Following Reactive Uptake of Ammonia, *Environ. Sci. Technol.*, 42, 793–799, 2008.
- Drewnick, F., Hings, S. S., DeCarlo, P. F., Jayne, J. T., Gonin, M., Fuhrer, K., Weimer, S., Jimenez, J. L., Demerjian, K. L., Borrmann, S., and Worsnop, D. R.: A New Time-of-Flight Aerosol Mass Spectrometer (ToF-AMS) - Instrument Description and First Field Deployment, *Aerosol Sci. Tech.*, 39, 637–658, 2005.
- DMT: Cloud Condensation Nuclei Counter Operator Manual DOC-0086 Revision A12, Droplet Measurement Technologies Inc., 2004.
- Dusek, U., Frank, G. P., Hildebrandt, L., Curtius, J., Schneider, J., Walter, S., Chand, D., Drewnick, F., Hings, S., Jung, D., Borrmann, S., and Andreae, M. O.: Size matters more than chemistry for cloud nucleating ability of aerosol particles, *Science*, 312, 1375–1378, 2006.
- Facchini, M. C., Decesari, S., Mircea, M., Fuzzi, S., and Loglio, G.: Surface Tension of Atmospheric Wet Aerosol and Cloud/Fog Droplets in Relation to their Organic Carbon Content and Chemical Composition, *Atmos. Environ.*, 34, 4853–4857, 2000.
- Giebl, H., Berner, A., Reischl, G., Puxbaum, H., Kasper-Giebl, A., and Hitzenberger, R.: CCN Activation of Oxalic and Malonic Acid Test Aerosols with the University of Vienna Cloud Condensation Nuclei Counter, *Aerosol Sci.*, 33, 1623–1634, 2002.
- Henning, S., Rosenoern, T., D'Anna, B., Gola, A. A., Svenningsson, B., and Bilde, M.: Cloud Droplet Activation and Surface Tension of Mixtures of Slightly Soluble Organics and Inorganic Salt, *Atmos. Chem. Phys.*, 5, 575–582, 2005, <http://www.atmos-chem-phys.net/5/575/2005/>.
- Hori, M., Ohta, S., Muraio, N., and Yamagata, S.: Activation Capability of Water Soluble Organic Substances as CCN, *Aerosol Sci.*, 34, 419–448, 2003.
- Huff Hartz, K. E., Tischuk, J. E., Chang, M. N., Chang, C. K., Donahue, M. N., and Pandis, S. N.: Cloud Condensation Nuclei Activation of Limited Solubility Organic Aerosol, *Atmos. Environ.*, 40, 605–617, 2005.
- IPCC: Climate Change 2007: The Physical Science Basis. Contribution of Working Group I to the Fourth Assessment Report of the Intergovernmental Panel on Climate Change, edited by: Solomon, S., Qin, D., Manning, M., Chen, Z., Marquis, M., Averyt, K.B., Tignor, M., and Miller, H. L., Cambridge University Press, Cambridge, United Kingdom and New York, NY, USA, 996 pp., 2007.
- Kaufman, Y. J. and Koren, I.: Smoke and Pollution Aerosol Effect on Cloud Cover, *Science*,

4465

- 313, 655–658, 2006.
- Kreidenweis, S. M., Petters, M. D., and DeMott, P. J.: Deliquescence-Controlled Activation of Organic Aerosols, *Geophys. Res. Lett.*, 33, L068801, doi:10.1029/2005GL024863, 2006.
- Kumar, P. P., Broekhuizen, K., and Abbatt, J. P. D.: Organic Acids as Cloud Condensation Nuclei: Laboratory Studies of Highly Soluble and Insoluble Species, *Atmos. Chem. Phys.*, 3, 509–520, 2003, <http://www.atmos-chem-phys.net/3/509/2003/>.
- Laaksonen, A., Korhonen, P., Kulmala, M., Charlson, R. J.: Modification of the Köhler Equation to Include Soluble Trace Gases and Slightly Soluble Substances, *J. Atmos. Sci.*, 55, 853–862, 1998.
- Lance, S., Medina, J., Smith, J. N., and Nenes, A.: Mapping the Operation of the DMT Continuous Flow CCN Counter, *Aerosol Sci. Tech.*, 40, 242–254, 2006.
- Lohmann, U. and Feichter, J.: Global Indirect Aerosol Effect: a Review, *Aerosol Chemistry and Physics*, 5, 715–737, 2005.
- McFiggans, G., Artaxo, P., Baltensperger, U., Coe, H., Facchini, M. C., Feingold, G., Fuzzi, S., Gysel, M., Laaksonen, A., Lohmann, U., Mentel, T. F., Murphy, D. M., O'Dowd, C. D., Snider, J. R., and Weingartner, E.: The effect of physical and chemical aerosol properties on warm cloud droplet activation, *Atmos. Chem. Phys.*, 6, 2593–2649, 2006, <http://www.atmos-chem-phys.net/6/2593/2006/>.
- Petters, M. D. and Kreidenweis, S. M.: A Single Parameter Representation of Hygroscopic Growth and Cloud Condensation Nucleus Activity, *Atmos. Chem. Phys.*, 7, 1961–1971, 2007, <http://www.atmos-chem-phys.net/7/1961/2007/>.
- Prenni, A. J., DeMott, P. J., Kreidenweis, S. M., Sherman, D. E., Russell, L. M., and Ming, Y.: The Effects of Low Molecular Weight Dicarboxylic Acids on Cloud Formation, *J. Phys. Chem A*, 105, 11 240–11 248, 2001.
- Pruppacher, H. R. and Klett, J. D.: *Microphysics of Clouds and Precipitation*, second ed., 714 pp., D. Reidel Publishing Company, Dordrecht, Holland, 1997.
- Raymond, T. M. and Pandis, S. N.: Formation of Cloud Droplets by Multicomponent Organic Particles, *J. Geophys Res.*, 108, doi:10.1029/2003JD003503, 2002.
- Rissman, T. A., Varutbangkul, V., Surratt, J. D., Topping, D. O., McFiggans, G., Flagan, R. C., and Seinfeld, J. H.: Cloud Condensation Nucleus (CCN) Behavior of Organic Aerosol Particles Generated by Atomization of Water and Methanol Solutions, *Atmos. Chem. Phys.*, 7, 2949–2971, 2007,

4466

- <http://www.atmos-chem-phys.net/7/2949/2007/>.
 Roberts, G.C., and Nenes, A.: A Continuous-Flow Streamwise Thermal-Gradient CCN Chamber for Atmospheric Measurements, *Aerosol Sci. Technol.*, 39, 206–221, 2005.
- Rose, D., Frank, G. P., Dusek, U., Gunthe, S. S., Andreae, M. O., and Pöschl, U.: Calibration and Measurement Uncertainties of a Continuous-Flow Cloud Condensation Nuclei Counter (DMT-CCNC): CCN Activation of Ammonium Sulfate and Sodium Chloride Aerosol Particles in Theory and Experiment, *Atmos. Chem. Phys. Discuss.*, 7, 8193–8260, 2007, <http://www.atmos-chem-phys-discuss.net/7/8193/2007/>.
- Saxena, P. and Hildemann, L.M.: Water-soluble organics in atmospheric particles: A critical review of the literature and application of thermodynamics to identify candidate compounds, *J. Atmos. Chem.*, 24, 57–109, doi:10.1007/BF00053823, 1996.
- Schwartz, S. E., Charlson, R. J., and Rhode, H.: Quantifying Climate Change – Too Rosy a Picture?, *Nature Reports Climate Change*, 2, 23–24, 2007.
- Shulman, M. L., Jacobson, M. C., Carlson, R. J., Synovec, R. E., and Young, T. E.: Dissolution Behavior and Surface Tension Effects of Organic Compounds in Nucleating Cloud Droplets, *Geophys. Res. Lett.*, 23, 277–280, 1996.
- Slowik, J. G., Stainken, K., Davidovits, P., Williams, L. R., Jayne, J. T., Kolb, C. E., Worsnop, D. R., Rudich, Y., DeCarlo, P. F., and Jimenez, J. L.: Particle Morphology and Density Characterization by Combined Mobility and Aerodynamic Diameter Measurements, Part 2: Application to Combustion-Generated Soot Aerosols as a Function of Fuel Equivalence Ratio, *Aerosol Sci. Technol.*, 38, 1206–1222, 2004.

4467

Table 1. Estimated particle dynamic shape factors as a function of particle size for dry adipic acid generated from homogeneous nucleation.

d_m	$\chi \pm \Delta\chi$
100	1.04±0.16
125	1.10±0.19
151	1.22±0.19
188	1.24±0.19
200	1.26±0.19

4468

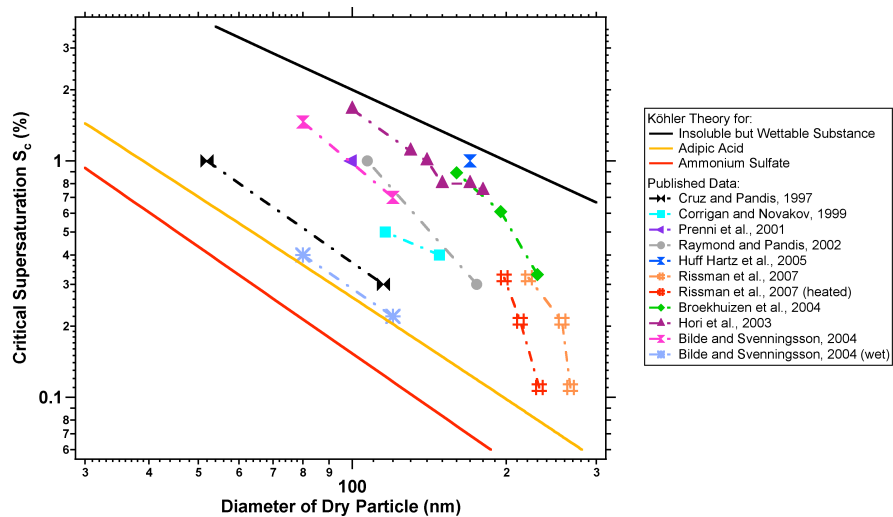


Fig. 1. Published critical supersaturations (S_c) for adipic acid as a function of dry particle size. Particles were obtained by atomizing aqueous solutions. The source of the data is shown by the symbols as identified in the insert. The state of the particles prior to activation was dry unless otherwise noted. Critical supersaturations predicted by the traditional Köhler theory are shown as solid lines for $(\text{NH}_4)_2\text{SO}_4$ (red line), adipic acid (orange line), and an insoluble but wettable substance (black line). See text for details.

4469

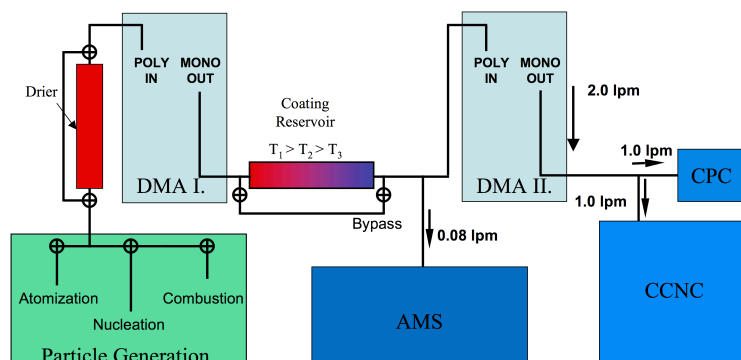


Fig. 2. Schematic of the experimental apparatus.

4470

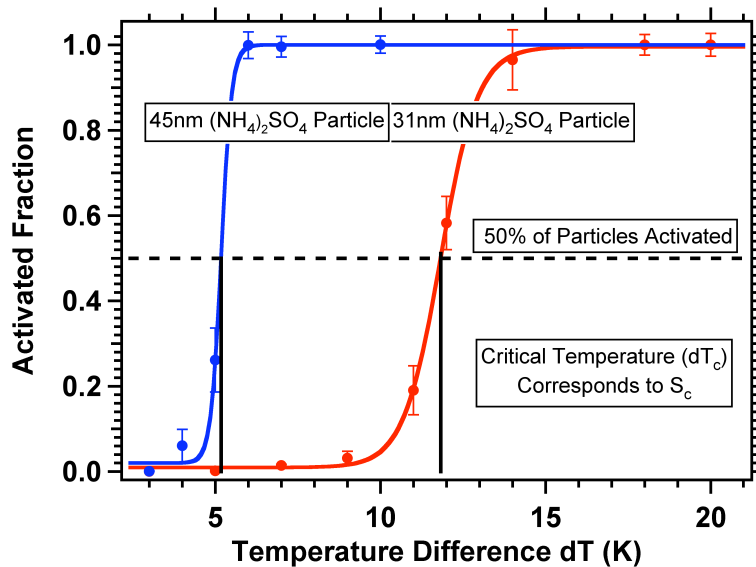


Fig. 3. Sample activation curves for 31 nm (red) and 45 nm (blue) ammonium sulfate particles. The critical supersaturation S_c calculated from the critical temperature dT_c is the supersaturation where 50% of the particles are activated.

4471

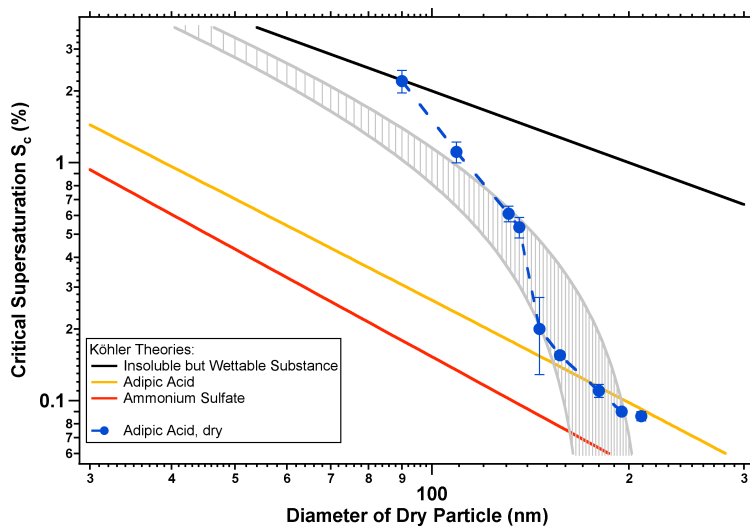


Fig. 4. S_c plotted as a function of particle diameter for dry adipic acid particles (blue symbols). Köhler theory lines are the same as in Fig. 1. The shaded area is the deliquescence region calculated from Eq. (A8) with $\gamma_w=0.990$. The upper and lower bounds correspond to solution surface tensions of 0.072 and 0.060 J/m², respectively.

4472

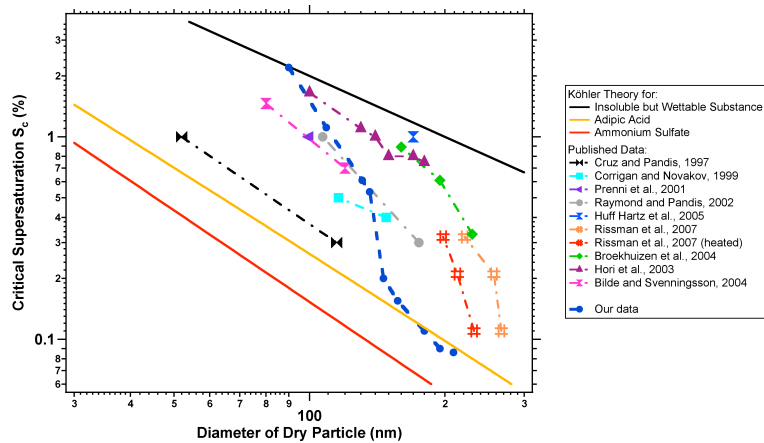


Fig. 5. S_c plotted as a function of particle diameter for dry adipic acid particles from previously published studies (as in Fig. 1) shown together with our measurements.

4473

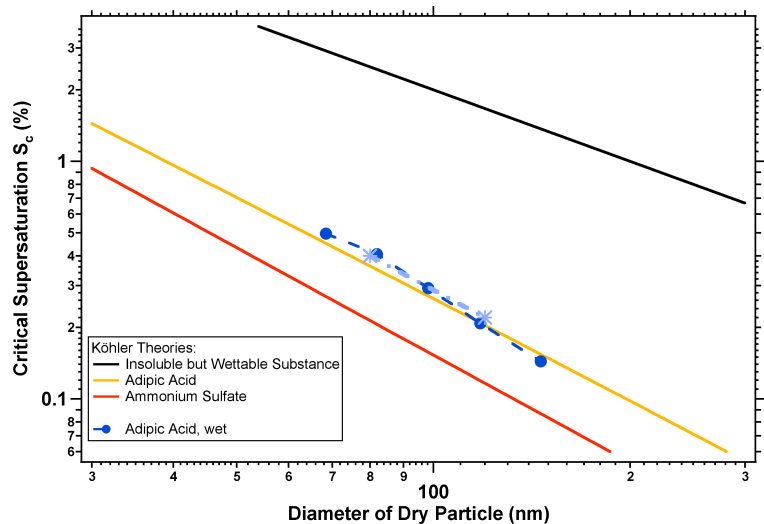


Fig. 6. S_c plotted as a function of particle diameter for wet adipic acid particles from our measurements (blue points) together with the data of Bilde and Svenningsson previously shown in Fig. 1.

4474

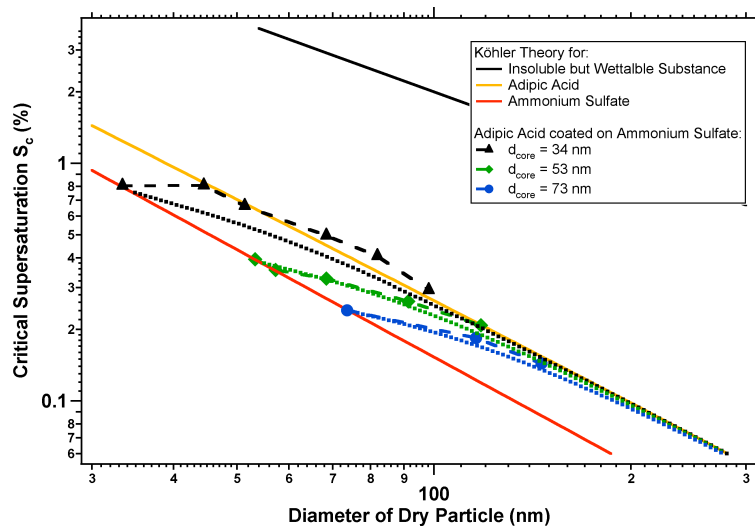


Fig. 7. S_c plotted as a function of particle diameter for adipic acid coated ammonium sulfate particles of sizes $d_{\text{core}}=34$ nm (black), 53 nm (green) and 73 nm (blue). The dashed lines are calculated using Köhler theory.

4475

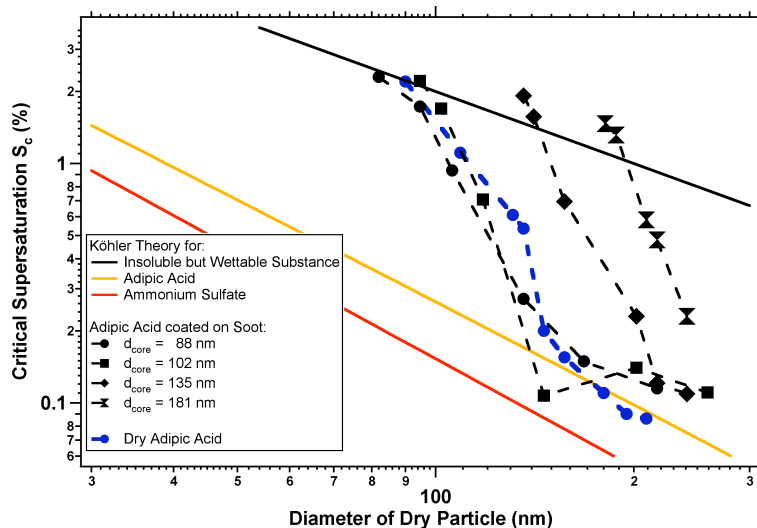


Fig. 8. S_c plotted as a function of particle diameter for adipic acid coated ammonium sulfate particles of sizes $d_{\text{core}}=88$ nm (diamonds), 102 nm (squares), 136 nm (triangles), and 181 nm (circles). Also included are the results for dry adipic acid derived during this study (blue).

4476

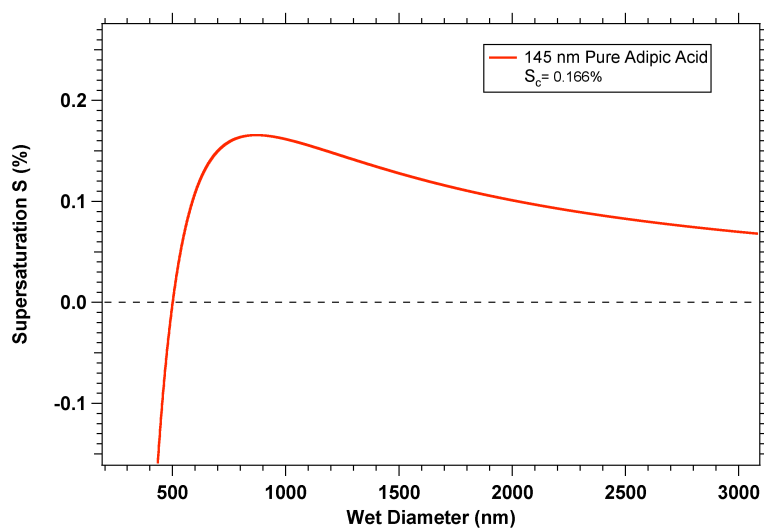


Fig. A1. Supersaturation S as a function of the wet particle diameter d_p for a particle composed of adipic acid. The adipic acid particle has dry diameter 145 nm and a critical supersaturation S_c of 0.166%.

4477

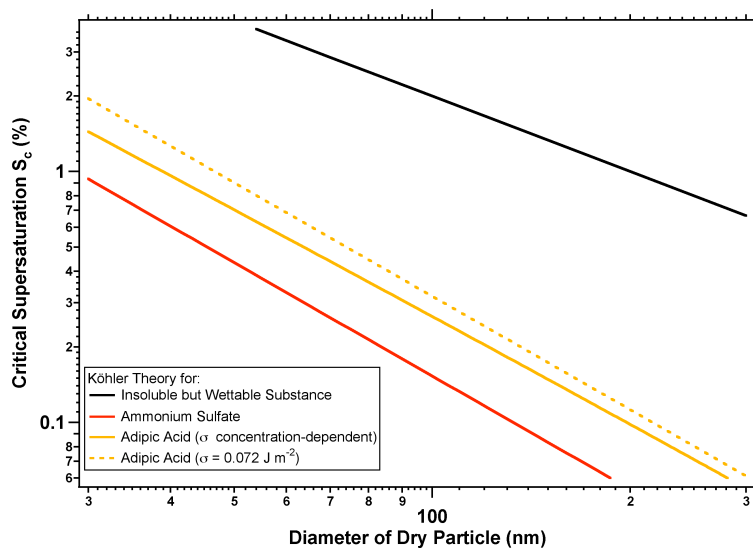


Fig. A2. Critical supersaturations as a function of initially dry particle diameter, calculated from Köhler theory for ammonium sulfate (red), adipic acid (yellow) and an insoluble but wettable substance (black). The lines for adipic acid have been modeled in two different ways: using the surface tension of water (dashed line) and using a concentration-dependent surface tension defined by the Szyszkowski-Langmuir equation (solid line). See text for details.

4478

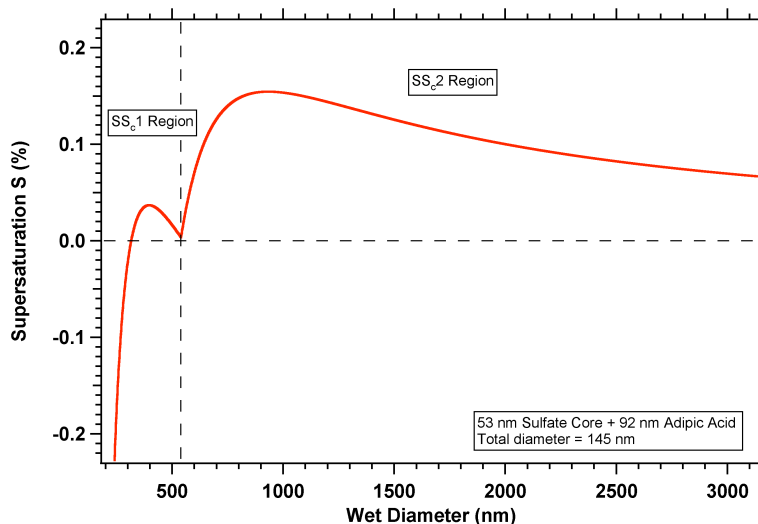


Fig. A3. Supersaturation as a function of wet particle diameter. Example of Köhler growth curve calculated using the modified Köhler theory for a particle composed of ammonium sulfate and adipic acid. The size of the ammonium sulfate core is 53 nm, the total diameter of the particle (ammonium sulfate + adipic acid) is 145 nm. In this case, the peak of the SS_{c1} regime is lower than that of the SS_{c2} regime, and the predicted critical supersaturation equals standard Köhler theory. That is, in this figure the S vs. d_p curve for wet diameters larger than 500 nm is identical to the function shown in Fig. A1 that models pure adipic acid of initial dry diameter = 145 nm.

4479

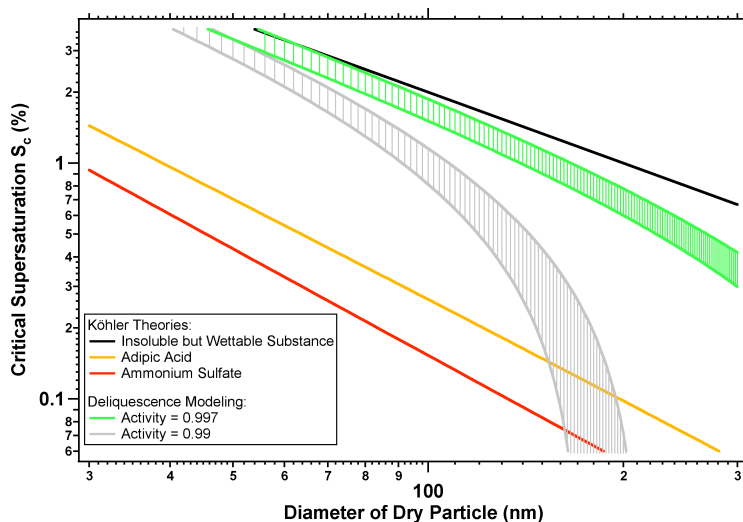


Fig. A4. Critical supersaturation S_c as a function of the dry particle diameter for adipic acid using water activities of 0.990 (gray) and 0.997 (green). The upper bound for each activity corresponds to a surface tension of 0.072 J/m^2 while the lower bound corresponds to a surface tension of 0.060 J/m^2 .

4480

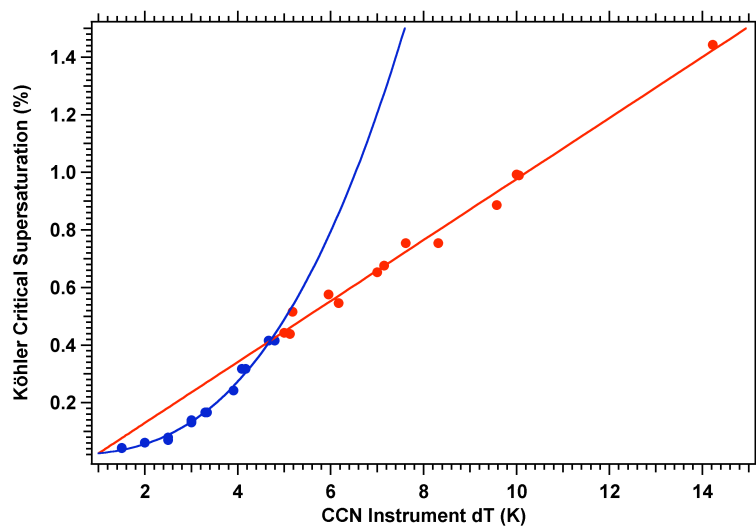


Fig. B1. Calculated critical supersaturation as a function of CCN instrument dT . The instrument flow rate was 0.93 L/min.

4481

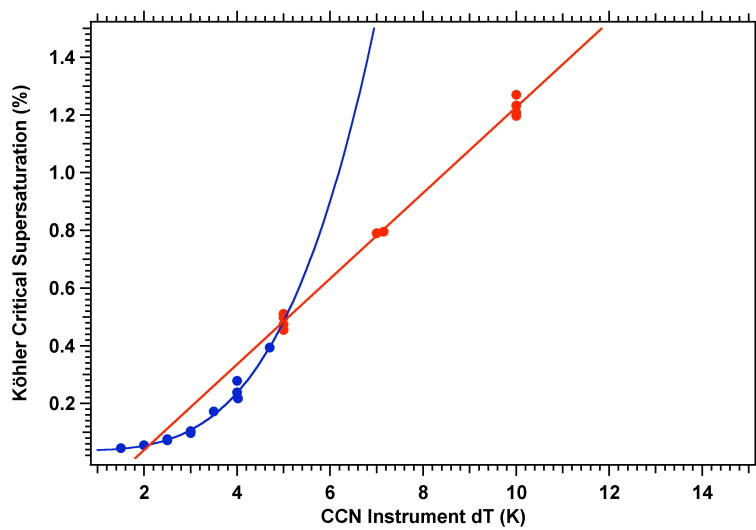


Fig. B2. Calculated critical supersaturation as a function of CCN instrument dT . The instrument flow rate was 1 L/min.

4482